

# THE INFLUENCE OF RUBBER CRUMBS ON THE CYCLIC DEFORMATION BEHAVIOUR OF WASTE MIXTURES

Yujie Qi<sup>1</sup>; Buddhima Indraratna<sup>2</sup>

<sup>1</sup>PhD, Research Associate, Centre for Geomechanics and Railway Engineering (CGRE), ARC Industry Transformation Training Centre for Advanced Rail Track Technologies (ITTC-Rail), School of Civil, Mining and Environmental Engineering, University of Wollongong, NSW 2522, Australia. Email: [qyujie@uow.edu.au](mailto:qyujie@uow.edu.au)

<sup>2</sup>MSc, DIC, PhD, FTSE, FIEAust, FASCE, FGS, Distinguished Professor, Research Director and Foundation Director, Civil Engineering, Centre for Geomechanics and Railway Engineering (CGRE), ARC Industry Transformation Training Centre for Advanced Rail Track Technologies (ITTC-Rail), Faculty of Engineering & Information Science, University of Wollongong, NSW 2522, Australia. Email: [indra@uow.edu.au](mailto:indra@uow.edu.au)

## ABSTRACT

The practical application of waste materials such as steel furnace slag (SFS) and coal wash (CW) is becoming more prevalent in many geotechnical projects. While the inclusion of rubber crumbs (RC) from recycled tyres into mixtures of SFS and CW not only solves the problem of large stockpiles of waste tyres, it can also provide an energy-absorbing medium that will reduce vibration and track degradation on railroads. However, the high compressibility of rubber materials may subject rail track systems to increased deformation if they are included, which is why an engineering insight into the effect that rubber crumbs have on the cyclic deformation of SFS+CW+RC mixtures is imperative. In this study the influence of RC composition on the cyclic deformation of rail subballast materials, i.e. total and resilient deformation, was investigated using drained cyclic triaxial tests. The results reveal that with the inclusion of RC, the total axial strain increases, the volumetric strain becomes more contractive, and the resilient deformation of the SFS+CW+RC mixture increases while its resilient modulus decreases. By comparing with traditional subballast, the waste mixture with 10% RC was found to be the optimal waste matrix for subballast in view of controlling deformation while maintaining sufficient resilient modulus.

## 1 INTRODUCTION

Coal mining and steel manufacturing are two of Australia's main industries, although the country benefits economically, there are problems with the large stockpiles of bi-product waste materials from the industrial processes. These waste materials occupy large storage areas which create environmental issues such as air and water pollution. The problems caused by these waste materials become more severe because their production rate far exceeds the rate at which they are processed. Of these waste materials, coal wash (CW) and steel furnace slag (SFS) are the main waste products. In Europe, around 12 million tonnes of steel slag are produced annually, of which more than 35% is disposed (Motz & Geiseler, 2001), whereas in New South Wales (Australia) more than 2 million tonnes of CW is produced per year, which is about 25-40% of the total production of raw coal (Lu and Do, 1992; Rujikiatkamjorn et al., 2013). Moreover, the ever increasing stockpile of waste tyres is creating another critical environmental problem in both developed and developing countries due to the rapidly increasing number of vehicles. It is estimated that 13.5 million tonnes of scrap tyres (United States 4.4 million tonnes; European Union 3.4 million tonnes; and the rest of the world 5.7 million tonnes) are generated every year (Rashad, 2016), while in Australia alone, more than 50 million tyre equivalent passenger units (EPU) of waste tyres are produced every year (Mountjoy et al., 2015). There is therefore an urgent need to recycle these waste materials. One efficient method is to utilise them in large civil engineering projects.

Although reusing these waste materials is both environmentally and economically attractive, they cannot be used individually in civil engineering projects due to their adverse geotechnical characteristics such as the swelling potential of SFS, the particle degradation of CW, and the high deformation of rubber; this is why previous studies mixed them with other materials to reduce their detrimental effects. SFS is usually mixed with Class C fly ash, cement, asphalt or concrete to be used in landfill, unbound pavements, road construction, and the production of cement (Yildirim and Prezzi, 2015; Xue et al., 2006; Juan et al., 2011). Coal washery rejects have been used in civil engineering projects such as road embankments, reclamation fill, asphalt aggregates, concrete aggregates and subgrade fill (Indraratna et al., 1994; Malasavage et al., 2012; Heitor et al., 2016). Since rubber materials have good geotechnical properties such as low unit weight, high hydraulic conductivity, and high damping property (Senetakis et al., 2012; Zheng and Kevin, 2000), past studies blended rubber crumbs (RC) which are derived from waste tyres with soil and used it in road construction, ground erosion control, slope stabilisation, landfill construction, and seismic isolation foundations (Lee, et al., 1999; Li et al.,

2016; Zheng and Sutter, 2000; Sheikh et al., 2013; Tsang et al., 2012). Moreover, to diminish the swelling potential of SFS and the collapse behaviour (particle degradation) of CW, past studies, i.e., Chiaro et al. (2013) and Tasalloti et al. (2015) mixed them together, and SFS+CW mixtures with a proper blending ratio have been successfully applied in port reclamation in Wollongong, Australia. Further, to extend the application of SFS+CW mixtures in dynamic loading projects, Indraratna et al. (2018) developed an energy absorbing layer for railway subballast by adding RC into the waste matrix.

Since excessive deformation will cause a hazardous impact to the foundation of a ballasted railway track, there is some concern with using RC in a railway foundation, albeit it will increase the damping ratio and energy absorbing capacity of the waste matrix (Indraratna et al., 2018; Qi et al., 2018a). This paper investigates the influence of RC content ( $R_b$ , %) on the deformation behaviour, i.e. total axial strain, total volumetric strain, and resilient strain, of SFS+CW+RC mixtures under cyclic loading. To achieve this goal a series of consolidated drained cyclic loading triaxial tests were carried out on SFS+CW+RC mixtures with SFS: CW = 7:3, and  $R_b = 0, 10, 20, 30,$  and 40%. A comparison between the deformation of traditional subballast and the waste matrix is also studied.

## 2 MATERIALS AND TEST PROGRAM

The source materials of SFS and CW are from Australia Steel Milling Services (ASMS) and Illawarra Coal Mining, respectively. The RC shredded from waste tyres used in this study is provided by Tyre Crumb Australia, and three different sizes (0-2.3mm, 0.3-3mm, and 1-7 mm) were used. The particle size distribution (PSD) curves of SFS, CW, and RC are shown in Figure 1. The dry method was used to sieve SFS and RC, whereas the wet method was used for CW because some fine particles adhered to the larger particles. SFS and CW are classified (unified soil classification system) as well-graded gravel with silty-sand (GW-GM), and well-graded sand with gravel (SW), respectively, whereas RC is referred to as granulated rubber (ASTM D6270, 2008).

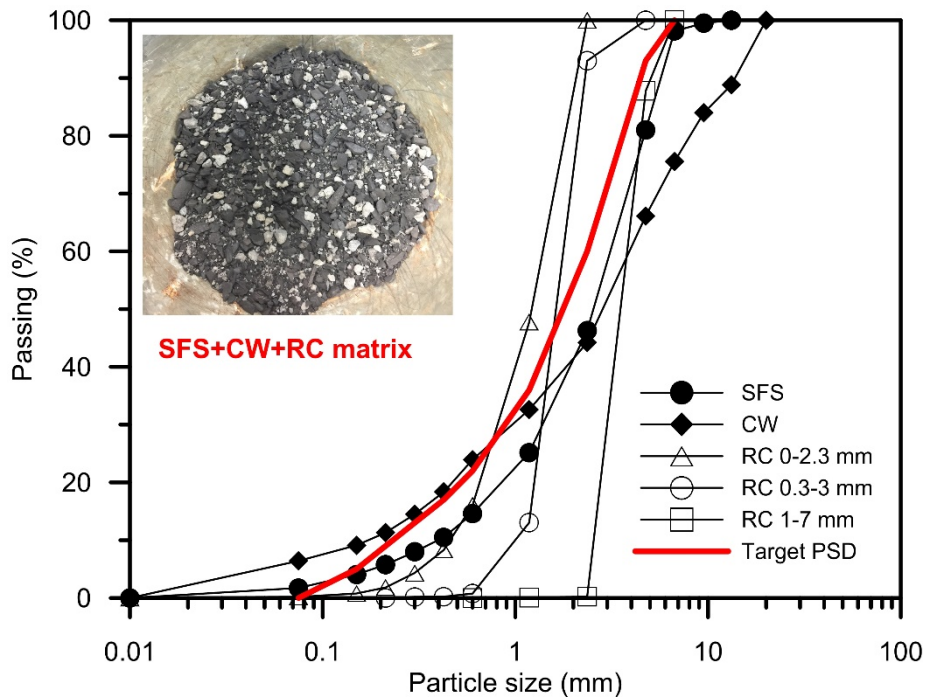


**Figure 1: PSD of SFS, CW, RC, and the target PSD for the waste matrix**

To prevent the influence of gradation, all the waste mixtures were mixed with the same PSD (the target PSD, Figure 1) chosen by Indraratna et al. (2018) on the basis of traditional subballast gradation in Australia. All the waste mixtures were blended by weight, because by-weight percentage is more accurate during sample preparation (Edil and Bosscher, 1994; Zheng and Kiven, 2000). The blending ratio of SFS: CW was set as 7:3 because this blending ratio imparts the waste matrix with the qualities of less particle degradation and acceptable volumetric expansion while maintaining sufficient shear strength (Indraratna et al., 2018; Qi et al., 2018b). The amount of RC in the matrix was not more than 40% to prevent the sample skeleton from being totally controlled by RC (Senetakis et al., 2012; Kim et al., 2008). The appearance of the SFS+CW+RC mixture with SFS: CW = 7:3, and 10% RC is shown in Figure 1.

A series of stress-controlled drained cyclic triaxial tests were carried out on the waste matrix by following the procedure suggested by ASTM D5311/D5311M (2013). The specimen was 100 mm high and 50 mm in diameter and was compacted

in three layers. All the specimens were prepared at optimum moisture content and compacted to 95% of their maximum dry density. The effective confining pressures ( $\sigma'_3$ ) used for the cyclic loading triaxial tests were 10, 40, and 70 kPa. The maximum deviator stress  $q_{max}$  is determined by using the cyclic stress ratio ( $CSR = \frac{q_{max}}{2\sigma'_3}$ )  $CSR = 0.8$  and the effective confining pressure. All of the abovementioned conditions for specimens and triaxial tests were used to simulate the field conditions of railway subballast.

The cyclic loading triaxial tests were carried out in three stages; saturation, consolidation, and cyclic loading. The specimen was saturated using back pressure and this stage was completed when the Skempton's B value exceeded 0.98. After saturation, the consolidation stage continued using the desired effective confining pressure (i.e.  $\sigma'_3 = 10, 40,$  or  $70 \text{ kPa}$ ) until unnoticeable change in volumetric strain was observed. Cyclic loading was applied using the frequency  $f = 5 \text{ Hz}$  to simulate the quasi-static condition which is usually used in track design procedures; cyclic loading stage was continued for 50,000 cycles.

### 3 TEST RESULTS

#### 3.1 TOTAL AXIAL STRAIN AND VOLUMETRIC STRAIN

The deformation of soil under cyclic loading can be characterised by permanent (plastic) strain and resilient (recoverable elastic) strain. The sum of permanent strain and resilient strain is the total strain. The definitions of total axial strain, permanent axial strain, and recoverable axial strain  $\epsilon_{1,rec}$  are shown in Figure 2. The permanent axial strain and resilient axial strain can both be reflected by the hysteretic cycles. Figure 3 (a-b) shows the hysteretic cycles of SFS+CW+RC mixtures with  $R_b = 10\%$  and  $30\%$  tested under  $\sigma'_3 = 70 \text{ kPa}$ . Note that the permanent axial strain increases with the loading cycles but at a decreasing rate of accumulation, whereas the resilient axial strain decreases as the number of loading cycles increases and gradually stabilises after around 1000 cycles. Note that the maximum deviator stress increases within the first 1000 cycles because most of the densification occurs at the beginning of the test, and the desired maximum deviator stress is achieved after around 1000 cycles. Moreover, the permanent axial strain of the waste matrix with  $R_b = 30\%$  is much greater than with  $R_b = 10\%$  as more densification occurs with increasing RC content. The resilient strain also increases when  $R_b$  increases because as  $R_b$  increases the skeleton of the specimen gradually changes from SFS+CW to RC so the specimen behaves more like rubber and the strain will recover more during unloading.

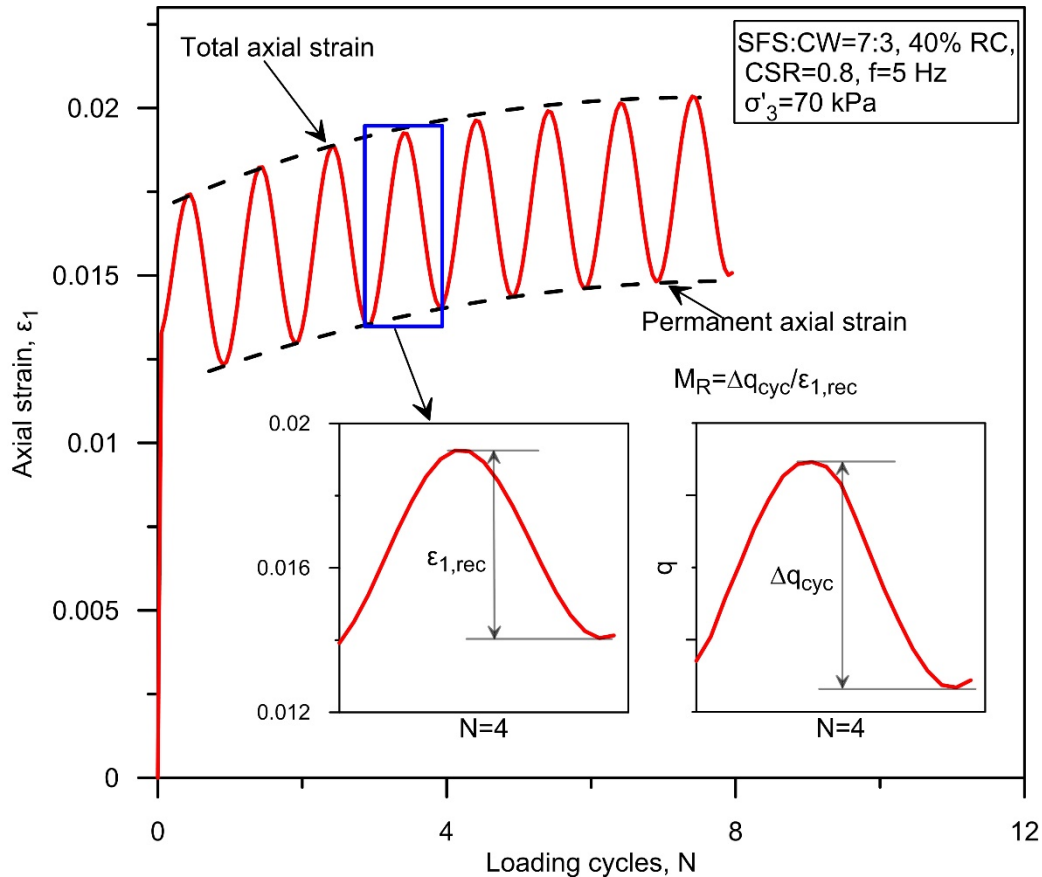
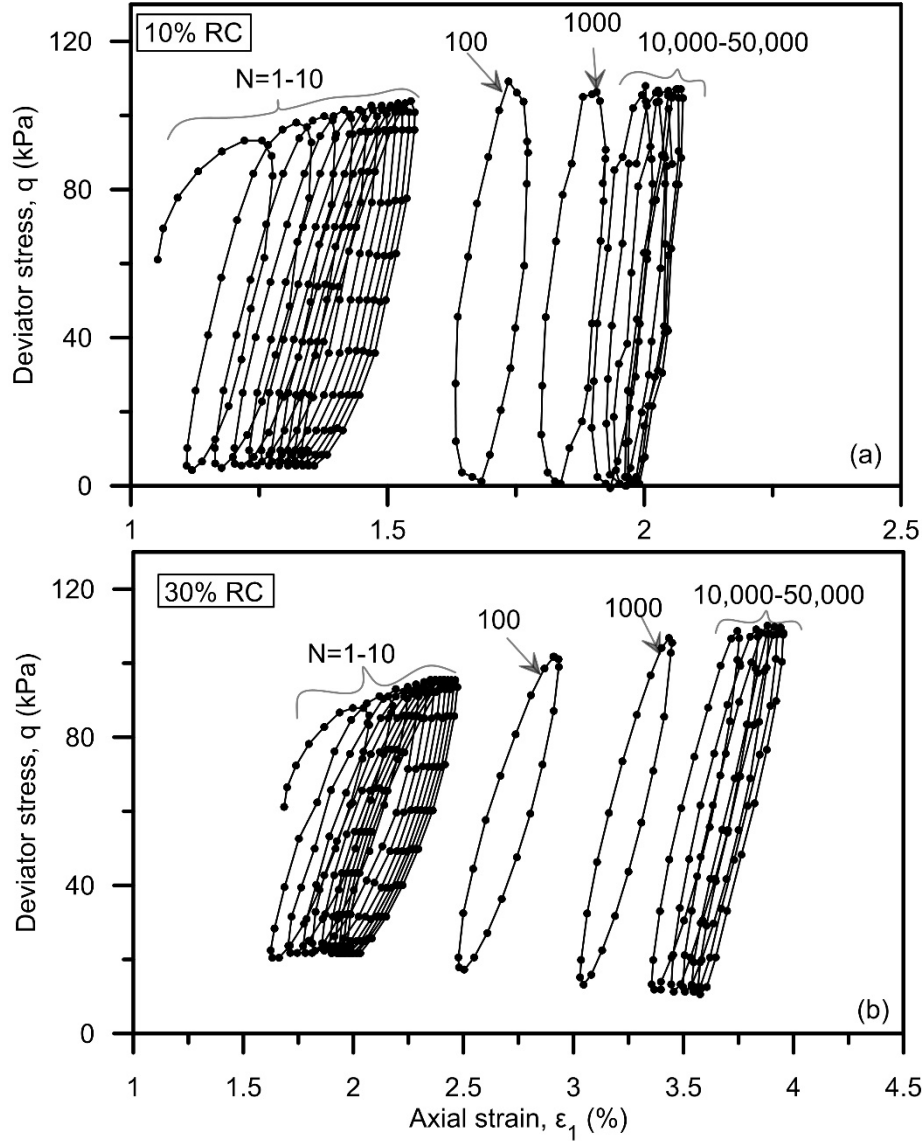


Figure 2: Definitions of total axial strain, permanent axial strain, recoverable axial strain and resilient modulus



**Figure 3: Hysteretic cycles of SFS+CW+RC mixtures with (a)  $R_b = 10\%$  and (b)  $R_b = 30\%$  tested with  $f=5$  Hz and  $\sigma'_3 = 70$  kPa**

The total axial strain and volumetric strain of SFS+CW+RC mixtures varying with the loading cycles are shown in Figure 4. It can be seen that under the same effective confining pressure, when  $R_b$  increases the axial strain increases and the volumetric strain becomes much more contractive. The axial strain and volumetric strain of the waste matrix with  $R_b \leq 10\%$  stabilises at around 10,000 cycles, which achieves shakedown. Here, ‘shakedown’ is a physical phenomenon of granular materials under cyclic loading that can be achieved when the axial strain of the granular materials stabilises after a certain period of time, or certain number of loading cycles (Indraratna et al., 2011). For the waste matrix with  $R_b \geq 20\%$  the axial strain continues to increase after 10,000 cycles, albeit this rate is marginal, and the volume of the specimens continues to compress to the end of the test. The influence of effective confining pressure on the total axial strain and volumetric strain is shown in Figure 4 (c-d); note that for the same waste matrix, the axial strain and volumetric strain increase as  $\sigma'_3$  increases. Under  $\sigma'_3 = 10 - 70$  kPa, the waste matrix with  $R_b = 10\%$  is always contractive, and when  $\sigma'_3 = 10$  kPa, the volumetric strain is negligible.

### 3.2 RESILIENT MODULUS

The resilient axial strain (recoverable strain) can be evaluated by the resilient modulus  $M_R$  which is defined as (Figure 2):

$$M_R = \frac{\Delta q_{cyc}}{\varepsilon_{1,rec}} \quad (1)$$

where  $\Delta q_{cyc}$  is the difference between the maximum deviator stress and the minimum deviator stress;  $\varepsilon_{1,rec}$  is the recoverable strain (elastic axial strain) during loading and unloading.

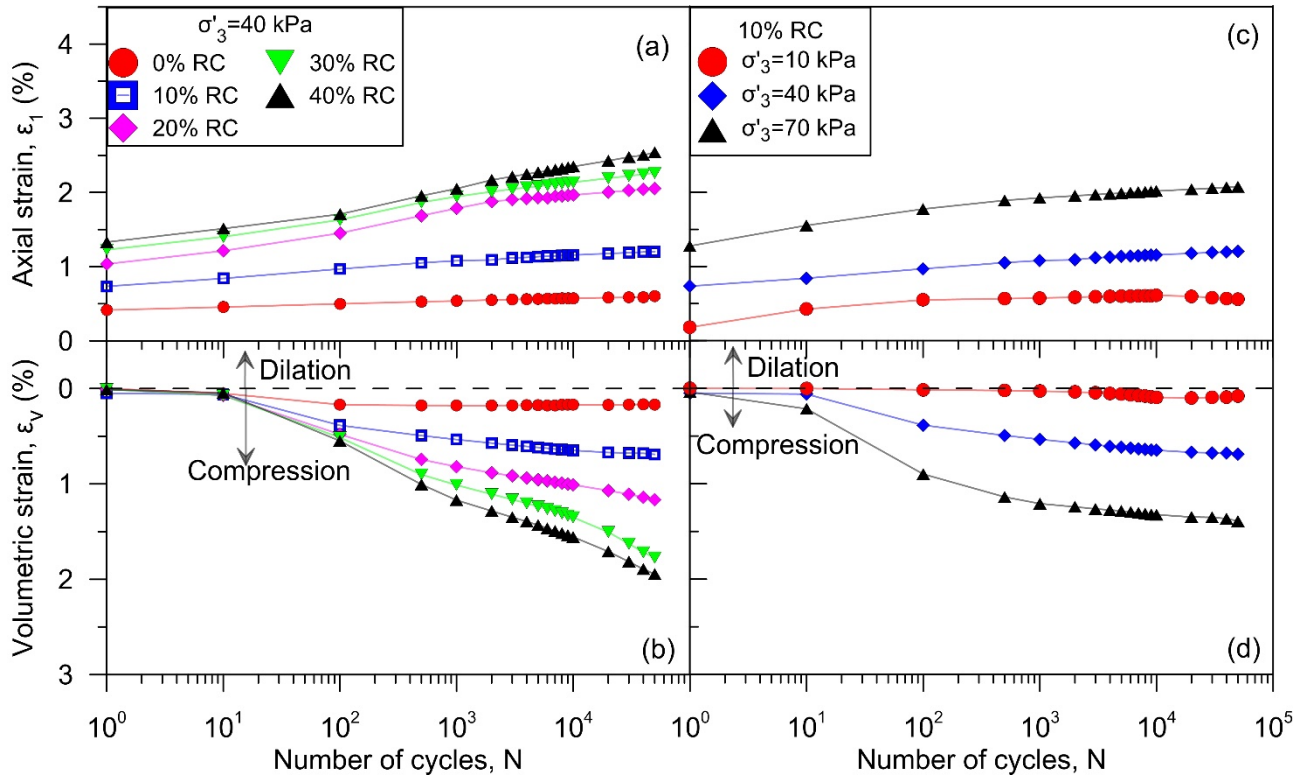


**Figure 4: Total axial strain and volumetric strain of SFS+CW+RC mixtures varying with loading cycles (modified after Qi et al., 2018b)**

To eliminate any influence of the irregularity in loading that might have occurred in the initial stage,  $M_R$  was determined after 1000 cycles where the maximum deviator stress was stable and more than 90% of permanent axial strain was generated (Figure 3). This agrees with previous studies by Nazzal and Mohammad (2010) and Lackenby et al. (2007). It can be seen that the magnitude of  $M_R$  increases slowly as the number of loading cycles increases, and then stabilises after 10,000 cycles (Figure 5a). Under the same effective confining pressure ( $\sigma'_3 = 40 \text{ kPa}$ )  $M_R$  decreases as RC is added, due to the larger recoverable axial strain generated by the addition of more RC (Figure 3). Moreover,  $M_R$  increases as  $\sigma'_3$  increases (Figure 5b). This is because when  $\sigma'_3$  increases, the RC becomes more compressible, more contacts between stiffer particles (SFS and CW) is forming, and the skeleton of the specimen becomes much stiffer, so less recoverable axial strain is generated.

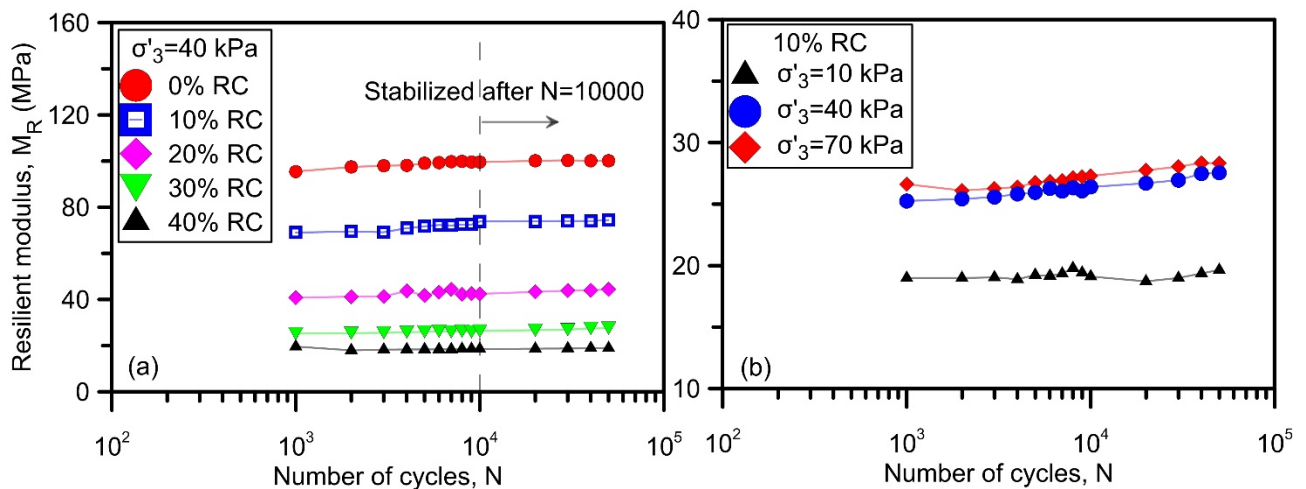


**Figure 5: Resilient modulus of SFS+CW+RC mixtures varying with loading cycles (modified after Qi et al., 2018b)**

### 3.3 EMPIRICAL RELATIONSHIPS BETWEEN STRAINS, $\sigma'_3$ , AND $R_b$

The influence of  $R_b$  on the cyclic deformation behaviour of the SFS+CW+RC mixtures can be better evaluated by plotting the total axial strain, total volumetric strain, and resilient modulus at 50,000 cycles (Figure 6 a-c) where the strain tends to be more stable. Note that the total  $\varepsilon_1$ ,  $\varepsilon_v$ , and  $M_R$  increase as  $\sigma'_3$  increases, while with the inclusion of RC  $\varepsilon_1$  and  $\varepsilon_v$  increase while  $M_R$  decreases. To prevent a hazardous impact to a ballast track foundation by excessive settlement, the total axial strain of the waste matrix should less than 2% under around  $\sigma'_3 = 40 \text{ kPa}$  (Teixeira et al., 2006; Figure 6a). Therefore, the axial strain of cyclic loading tests indicates that RC contents in the waste matrix should be less than 20%. Moreover, the materials that dilate under cyclic loading should be avoided to be used as subballast, and therefore a waste matrix without RC should not be used as subballast (Figure 6b). Furthermore, the resilient modulus for subballast is expected to be in the range 60 kPa to 80 kPa, as suggested by Shahu et al. (1999), so the resilient modulus of the waste matrix obtained from the cyclic loading tests shown in Figure 6 (c) indicates that a waste matrix with 10% RC is suitable for subballast.

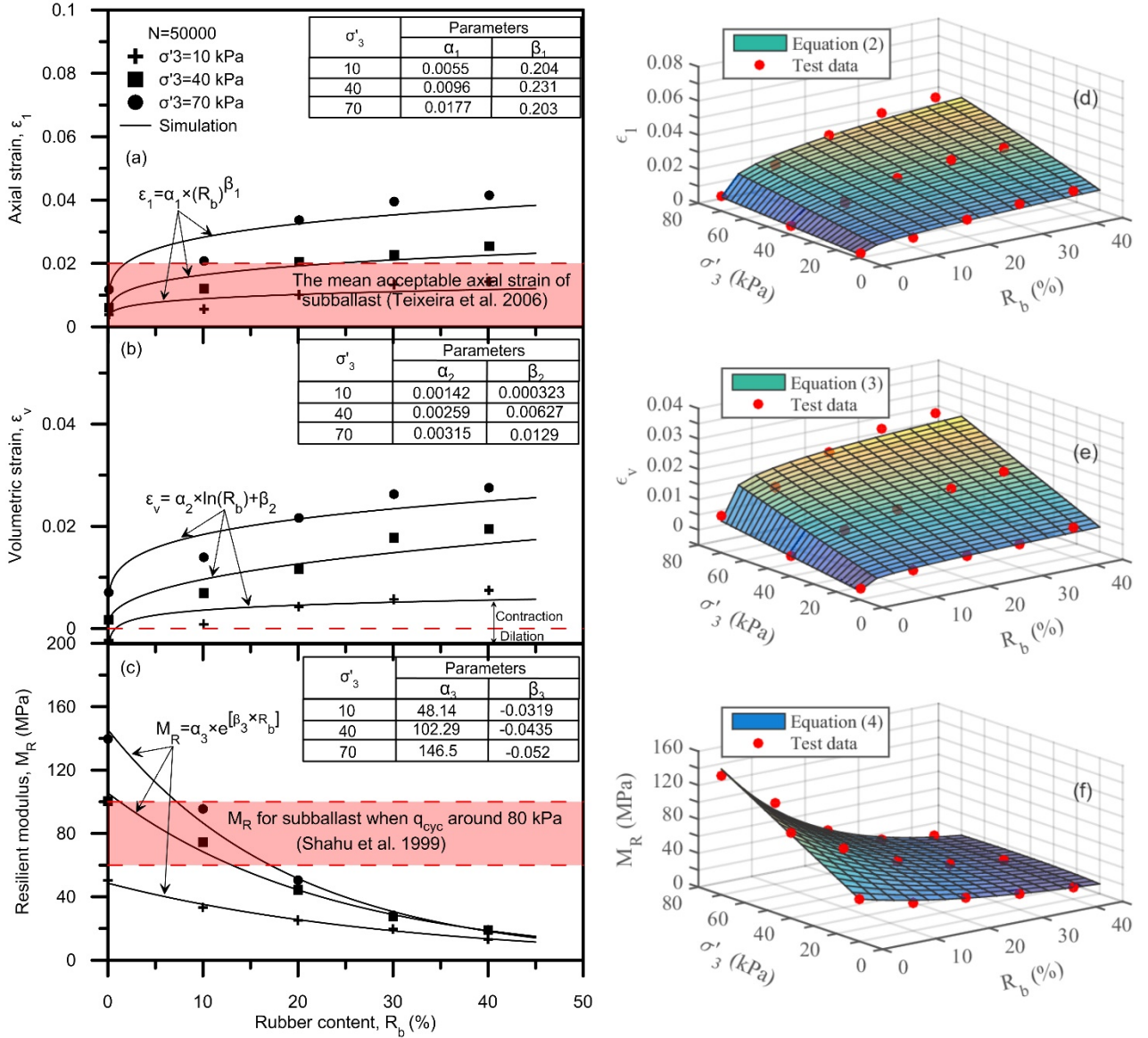


**Figure 6: (a-c) Total axial strain, total volumetric strain and resilient modulus for SFS+CW+RC mixtures at 50,000 cycles; (d-e) 3-D plot of relationships between  $\sigma'_3$ ,  $R_b$  and  $\varepsilon_1$ ,  $\varepsilon_v$ , and  $M_R$  (modified after Qi et al., 2018b)**

It is interesting to find that the influence of  $\sigma'_3$  and  $R_b$  on  $\varepsilon_1$ ,  $\varepsilon_v$ ,  $M_R$  can be reflected by the empirical equations:

$$\varepsilon_1 = \alpha_1 \times (R_b)^{\beta_1} = (a_1 \times \sigma'_3 + b_1) \times (R_b)^{a_2 \times \sigma'_3 + b_2} \quad (2)$$

$$\varepsilon_v = \alpha_2 \times \ln(R_b) + \beta_2 = (a_3 \times \sigma'_3 + b_3) \times \ln(R_b) + (a_4 \times \sigma'_3 + b_4) \quad (3)$$

$$M_R = \alpha_3 \times e^{\beta_3 \times R_b} = (a_5 \times \sigma'_3 + b_5) \times e^{(a_6 \times \sigma'_3 + b_6) \times R_b} \quad (4)$$

where  $\alpha_i$  and  $\beta_i$  ( $i = 1, 2, 3$ ) are calibration parameters. The value of  $\alpha_i$  and  $\beta_i$  are shown in Figure 6 (a-c), and both  $\alpha_i$  and  $\beta_i$  have a linear relationship with  $\sigma'_3$ , as is also reflected in Equations (2-4).  $a_i$  and  $b_i$  ( $i = 1, 2, 3, 4, 5, 6$ ) are also calibration parameters, and their values are shown in Table 1. To better illustrate the empirical relationship between  $\sigma'_3$  and  $R_b$  and  $\varepsilon_1$ ,  $\varepsilon_v$ ,  $M_R$ , the test data and Equations (2-4) are plotted in a 3-D space (Figure 6 d-e). The curved surfaces of  $\varepsilon_1$ ,  $\varepsilon_v$ , and  $M_R$  are formed by the influence of  $\sigma'_3$  and  $R_b$ . Note that the simulated results by Equations (2-4) match the test results very well.

**Table 1: The value of  $a_i$  and  $b_i$**

$i$	$a_i$	$b_i$
1	$1.7 \times 10^{-4}$	$-4.17 \times 10^{-4}$
2	$2.28 \times 10^{-3}$	0.283
3	$3.7 \times 10^{-5}$	$2.1 \times 10^{-4}$
4	$4.8 \times 10^{-4}$	$2.2 \times 10^{-3}$
5	1.639	$-3.35 \times 10^{-4}$
6	33.4	-0.0291

## 4 CONCLUSIONS

In this paper a series of stress-controlled cyclic triaxial tests have been carried out on SFS+CW+RC mixtures with SFS:CW = 7:3 and  $R_b = 0 - 40\%$  to investigate the influence of  $R_b$  and  $\sigma'_3$  on the cyclic deformation behaviour of the waste matrix. The test results indicate that:

- (1) As  $R_b$  and  $\sigma'_3$  increase, the total axial strain increases and the volumetric strain of the waste matrix becomes much more contractive. All the waste matrix samples show contractive behaviour, although the waste mixture without RC dilates under very low effective confining pressure (i.e.,  $\sigma'_3 = 10 \text{ kPa}$ ). The axial strain and volumetric strain increase as the number of loading cycles increases, and the trend of the increasing rate stabilises after  $N = 10,000$ .
- (2) The magnitude of  $M_R$  decreases as  $R_b$  increases, but it decreases when  $\sigma'_3$  increases.  $M_R$  is determined after  $N = 1000$ , while the value of  $M_R$  increases very slowly as the number of loading cycles increases, but it gradually stabilises after  $N = 10,000$ .
- (3) The empirical relationships between  $\sigma'_3$ ,  $R_b$  and  $\varepsilon_1$ ,  $\varepsilon_v$ , and  $M_R$  have been established, and there is a good agreement between the prediction and the measured data.
- (4) Compared to traditional subballast, a waste matrix with 10% RC can be used as subballast because it has less axial strain and volumetric strain, and it has an acceptable resilient modulus; moreover, it can achieve a shakedown condition at around 10,000 cycles.

## ACKNOWLEDGEMENTS

The first author would like to acknowledge the financial assistance provided by the Australian Research Council Discovery Project (ARC-DP) and ARC Industry Transformation Training Centre for Advanced Rail Track Technologies (ITTC-Rail). The assistance provided by industry (ASMS, South 32, and Tyre Crumb Australia) in relation to the procurement of material used in this study is gratefully acknowledged. The assistance in the laboratory from Mr. Richard Berndt and the occasional technical feedback from A/Professor Cholachat Rujikiatkamjorn are appreciated. Some figures in this paper were modified after Qi et al. (2018b) whereby the original data has been reproduced with kind permission from ASCE: Journal of Geotechnical and Geoenvironmental Engineering.

## REFERENCES

- ASTM D5311/D5311M - 13, American Society for Tests and Materials 2008 (R2012), Standard test method for load controlled cyclic triaxial strength of soil, ASTM International, West Conshohocken, PA, USA.
- ASTM D6270, American Society for Tests and Materials 2008 (R2012), Standard practice for use of scrap tyres in civil engineering applications, ASTM D International, West Conshohocken, PA, USA.
- Chiaro, G., Indraratna, B., Tasalloti, S.M.A. and Rujikiatkamjorn, C. (2015). "Optimisation of coal wash-slag blend as a structural fill." *Proc. ICE: Ground Improvement*, 168(GI1), 33-44.
- Edil, T. and Bosscher, P. (1994). "Engineering properties of tyre chips and soil mixtures." *Geotechnical Testing Journal*, 17(4), 453-464.

- Heitor, A., Indraratna, B., Kaliboullah, C., Rujikiatkamjorn, C., and McIntosh, G. (2016). "Drained and undrained shearing behavior of compacted coal wash." *J. Geotech. Geoenviron. Eng.*, 142(5), 04016006.
- Indraratna, B., Gasson, I., and Chowdhury, R. N. (1994). "Utilization of compacted coal tailings as a structural fill." *Can. Geotech. J.*, 31(5), 614–623.
- Indraratna, B., Salim, W. and Rujikiatkamjorn, C. (2011). *Advanced rail geotechnology – ballasted track*, CRC Press/Balkema, The Netherlands.
- Indraratna, B., Qi, Y., and Heitor, A. (2018). "Evaluating the Properties of Mixtures of Steel Furnace Slag, Coal Wash, and Rubber Crumbs Used as Subballast." *J. Mater. Civil Eng.*, 30(1), 04017251.
- Juan, L.M., Claisse, P. and Ganjian, E. (2011). "Effect of steel slag and Portland cement in the rate of hydration and strength of blast furnace slag pastes." *J. Mater. Civ. Eng.*, 23(2), 153-160.
- Kim, H.K. and Santamarina, J.C. (2008). "Sand-rubber mixtures (large rubber chips)." *Can. Geotech. J.*, 45(10), 1457-1466.
- Lackenby, J., Indraratna, B., McDowell, G. and Christie, D. (2007). "Effect of confining pressure on ballast degradation and deformation under cyclic triaxial loading." *Géotechnique*, 57(6), 527-536.
- Lee, J.H., Salgado, R., Bernal, A., and Lovell, C.W. (1999). "Shredded tires and rubber-sand as lightweight backfill." *J. Geotech. Geoenviron. Eng.*, 125(2), 132-141.
- Li, B., Huang, M. S., and Zeng, X. W. (2016). "Dynamic behavior and liquefaction analysis of recycled-rubber sand mixtures." *J. Mater. Civil Eng.*, 28(11), 04016122.
- Lu, G.Q. and Do, D.D. (1992). "Physical structure and adsorption properties of coal washery reject." *Fuel*, 71(7), 809-813.
- Malasavage, N., Jagupilla, S., Grubb, D., Wazne, M., and Coon, W. (2012). "Geotechnical Performance of Dredged Material—Steel Slag Fines Blends: Laboratory and Field Evaluation." *J. Geotech. Geoenviron. Eng.*, 138(8), 981-991.
- Motz, H. and Geiseler, J. (2001). "Products of steel slags an opportunity to save natural resources." *Waste Management*, 21(3), 285-293.
- Mountjoy, E., Hasthanayake, D., Freeman, T. (2015). "Stocks & Fate of End of Life Tyres - 2013-14 Study—Final Report." <http://www.nepc.gov.au/resource/stocks-and-fate-end-life-tyres-2013-14-study>.
- Nazzal, M.D. and Mohammad, L.N. (2010). "Estimation of resilient modulus of subgrade soils for design of pavement structures." *J. Mater. Civil Eng.*, 22(7), 726- 734.
- Qi, Y., Indraratna, B., Heitor, A., Vinod, J.S. (2018a). "The Influence of Rubber Crumbs on the Energy Absorbing Property of Waste Mixtures." Proceedings of the International Symposium on Geotechnics of Transportation Infrastructure (ISGTI 2018). New Delhi, India. pp. 455-460.
- Qi, Y., Indraratna, B., Heitor, A., and Vinod, J.S. (2018b). "Effect of Rubber Crumbs on the Cyclic Behaviour of Steel Furnace Slag and Coal Wash Mixtures." *J. Geotech. Geoenviron. Eng.*, 144(2), 04017107.
- Rashad, A.M. (2016). "A comprehensive overview about recycling rubber as fine aggregate replacement in traditional cementitious materials." *International Journal of Sustainable Built Environment*, 5(1), 46-82.
- Rujikiatkamjorn, C., Indraratna, B., and Chiaro, G. (2013). "Compaction of coal wash to optimise its utilisation as water-front reclamation fill." *Geomechanics Geoengineering*, 8(1), 181-212.
- Senetakis, K., Anastasiadis, A. and Pitolakis, K. (2012). "Dynamic properties of dry sand/rubber (SRM) and gravel/rubber (GRM) mixtures in a wide range of shearing strain amplitudes." *J. Soil Dyn. Earthquake Eng.*, 33(1), 38-53.
- Shahu, J.T., Kameswara Rao, N.S.V. and Yudhbir (1999). "Parametric study of resilient response of tracks with a sub-ballast layer." *Can. Geotech. J.*, 36(6), 1137-1150.
- Sheikh, M. N., Mashiri, M.S., Vinod, J.S., and Tsang, H.H. (2013). "Shear and compressibility behavior of sand-tire crumb mixtures." *J. Mater. Civil Eng.*, 25(10), 1366–1374.
- Tasalloti, S.M.A., Indraratna, B., Rujikiatkamjorn, C., Heitor, A. and Chiaro, G. (2015). "A laboratory study on the shear behavior of mixtures of coal wash and steel furnace slag as potential structural fill." *Geotechnical testing journal*, 38(4), 361-372.
- Teixeira, P.F., López-Pita, A., Casas-Esplugas, C., Bachiller, A. and Robusté, F. (2006). "Improvements in high-speed ballasted track design: Benefits of bituminous subballast layers." *Transportation Research Record* 1943, 43-49.
- Tsang, H. H., Lo, S. H., Xu, X., and Sheikh, M. N. (2012). "Seismic isolation for low-to-medium-rise buildings using granulated rubber-soil mixtures: Numerical study." *Earthquake Eng. Struct. Dyn.*, 41(14), 2009-2024.
- Xue, Y., Wu, S., Hou, H. and Zha, J. (2006). "Experimental investigation of basic oxygen furnace slag used as aggregate in asphalt mixture." *J. Hazard. Mater.*, 138(2), 261–268.
- Yildirim, I.Z. and Prezzi, M. (2015). "Geotechnical properties of fresh and aged basic oxygen furnace steel slag." *J. Mater. Civil Eng.*, 27(12), 04015046-1-11.
- Zheng, Y.F. and Sutter, K.G. (2000). "Dynamic properties of granulated rubber/sand mixtures." *Geotechnical Testing Journal*, 23(3), 338-344.